



Mechanics of fish skin: A computational approach for bio-inspired flexible composites



Franck J. Vernerey^{a,c,*}, Kamtornkiat Musiket^a, Francois Barthelat^b

^a Department of Civil, Environmental and Architectural Engineering, University of Colorado, Boulder, USA

^b Department of Mechanical Engineering, McGill University, Montreal, Canada

^c Program of Material Science and Engineering, University of Colorado, Boulder, USA

ARTICLE INFO

Article history:

Received 11 January 2013

Received in revised form 1 August 2013

Available online 15 October 2013

Keywords:

Bio-inspired membranes

Thin shells

Computational homogenization

Biomaterials

ABSTRACT

Natural materials and structures are increasingly becoming a source of inspiration for the design novel of engineering systems. In this context, the structure of fish skin, made of an intricate arrangement of flexible plates growing out of the dermis of a majority of fish, can be of particular interest for materials such as protective layers or flexible electronics. To better understand the mechanics of these composite shells, we introduce here a general computational framework that aims at establishing a relationship between their structure and their overall mechanical response. Taking advantage of the periodicity of the scale arrangement, it is shown that a representative periodic cell can be introduced as the basic element to carry out a homogenization procedure based on the Hill-Mendel condition. The proposed procedure is applied to the specific case of the fish skin structure of the *Morone saxatilis*, using a computational finite element approach. Our numerical study shows that fish skin possesses a highly anisotropic response, with a softer bending stiffness in the longitudinal direction of the fish. This softer response arises from significant scale rotations during bending, which induce a stiffening of the response under large bending curvature. Interestingly, this mechanism can be suppressed or magnified by tuning the rotational stiffness of the scale-dermis attachment but is not activated in the lateral direction. These results are not only valuable to the engineering design of flexible and protective shells, but also have implications on the mechanics of fish swimming.

Published by Elsevier Ltd.

1. Introduction

As a result of evolution, biological materials and structures often possess optimized properties and organizations (Vogel, 2000); this has made them a great source of inspiration for engineers seeking to develop novel materials with unprecedented performances. Biomimetics (the science of imitating nature (Vincent et al., 2006)) has recently been investigating a number of materials with remarkable properties (Meyers et al., 2006) such as seashells (Barthelat et al., 2007; Tang et al., 2003; Barthelat, 2012), glass sponge skeleton (Aizenberg et al., 2005), and toucan beaks (Meyers et al., 2006). A fundamental understanding of the relationship between structure and function of these high-performance biological materials has already given invaluable insight in how to design tomorrow's engineering materials.

The ultra-thin structure of fish skin is another example of a natural material that combines desirable mechanical properties such as compliance, resistance to penetration and lightweight

but surprisingly, it has received little attention from the materials development community. In a review article on mineralized tissues, Currey (1999) noted that some fish scales are so tough that they could not be fractured even after immersion in liquid nitrogen!". While the full range of this material's function is not known, it performs especially well in a variety of tasks. First, individual scales resist penetration and provide a physical barrier against attack from predator (Zhu et al., 2011; Bruet et al., 2008; Chen et al., 2011). At a larger length-scale, the arrangement of the scales provides a flexible skin that allows for changes in a fish shape during swimming. Indeed, in addition to its superior hydrodynamics properties (Sudo et al., 2002), the scaled skin has been shown to play a critical structural role in fish locomotion by regulating wave propagation (Long et al., 2002) and by acting as an external tendon (Hebrank, 1980; Hebrank and Hebrank, 1986). These multifunctional behaviors could not be achieved without the presence of highly organized structure across several length scales (Zhu et al., 2012), tailored to respond to environmental threats.

The scaled structure of fish skin seems to be optimized to provide resistance to penetration while retaining relative freedom of movement, features that are highly desirable for next generations of body armors. A systematic biomimetic "transfer of technology"

* Corresponding author.

E-mail address: franck.vernerey@colorado.edu (F.J. Vernerey).

from this material is therefore of interest, but requires a fundamental understanding of the mechanics of fish skin. In particular, the design of a fish skin targeted for specific applications necessitates the elaboration of experimental and computational approaches that can establish the structure–property relation of the material. Features to consider include for instance the stiffness and organic composition of the scales, the mechanical interactions between scales (via friction and contact), the nature of attachment of scales to the underlying dermis as well as their morphology, shape, size, and organization. As mentioned above, fish skin has a hierarchical organization which plays a crucial role in its overall mechanical performance. However the contribution and synergies of each scale has yet to be investigated. For example, while the source of toughness for a single scale and its modes of failure have been identified (Zhu et al., 2011; Chen et al., 2011) it is still not entirely clear how neighboring scales interact to prevent penetration and to minimize skin deflection.

To better understand the structure–property relationship of fish skin, we introduce here a general computational framework based on unit cell modeling and traditional homogenization. We particularly extend the traditional Hill–Mendel relation to derive a relationship between overall curvature and bending moments of a general class of composite thin shells. Taking advantage of the structural periodicity of fish-skin, we show that a representative periodic cell can be introduced as the basic element to carry out a homogenization procedure. The proposed procedure is then applied to two cases. First, we consider a type of fish skin that is characterized by a one-dimensional scale arrangement and that serves as a benchmark problem to verify the validity of our predictions. Second, we consider the specific case of the skin of the *Morone saxatilis* which is representative of a large variety of fish with teleost scales. For each example, we use the computational framework to elucidate how structure and material's response are related. Overall, the paper is organized as follows. The next section provides a general description of the structural organization of fish skin, discusses its mechanical role as a biological material and introduce a unit cell approach to represent the entire structure via a small periodic domain. Section 2 then lays out the proposed computational strategy to establish a link between properties and structure of fish scale composites. The approach is subsequently used in Section 3 in order to numerically determine the response (moment–curvature) of the two scale structures discussed above. A discussion of the results, followed by concluding remarks, is finally provided in Section 4.

2. Structure, mechanics and modeling of scaled skin

As presented in Fig. 1, we here concentrate on three distinct hierarchical length scales of fish-skin, ranging from the millimeter (size of a single scale) to several centimeters (size of a fish). The size and thickness of fish scales vary significantly across species (Jawad, 2005), and this very likely influences their overall mechanical performance. For example, the thickness and diameter of the scale influences the stresses resulting from a predator's bite, which in turn influences the overall strength of the scale (Chen et al., 2011). In case of a predator's attack, the scales act collectively to prevent penetration and minimize the deflection of the skin, and therefore delay damage to the underlying tissues. Important factors influencing the behavior at this level are the mechanical behavior of individual scale, the interactions between neighboring scales, as well as the behavior of the dermis that support the scales. It was shown in Vernerey and Barthelat (2010) that these factors drive the rotation of individual scales with respect to the underlying dermis (Fig. 1), a mechanism that controls the response of the skin during longitudinal bending. Besides its organized hierarchical

nature, the structure of fish scales is distinguished by the presence of both an organic and mineral phase.

The present work concentrates on a teleost fish, the *Morone saxatilis* (common name striped bass) as a model for scale geometry and arrangement. Indeed, while other scale types, such as ganoid and cosmoid, are usually stiffer and harder than teleost scales, they are currently found in only a few living fish species. Teleost scales have however largely prevailed over the course of evolution, and are now found in more than 99% of living species. This suggests that the lighter and thinner teleost scales may offer better trade-offs between swimming speed, agility and protection. The *Morone saxatilis* is characterized by its ctenoid scales, which have a spiny posterior margin, an overall circular shape and are comprised of two main layers: a layer of bony organic structure and an inner layer of collagen (Zhu et al., 2011). The imbricate pattern of ctenoid scales gives the fish greater flexibility than in fish with cosmoid and ganoid scales and often leads to unique combinations of stiffness, hardness and toughness (Vernerey and Barthelat, 2010; Zhu et al., 2012). Due to the variety of building blocks across length-scales, the mechanical properties of fish scale may be modified by slight changes at any level of its structure.

2.1. The mechanical role of scales: a simple experiment

Penetration tests, which essentially duplicate the biting attack of a predator, were performed on *Morone saxatilis* and the resulted load–deflection assessed. The tests consisted of driving a sharp needle ($\approx 30 \mu\text{m}$ tip radius) through the skin of a fish cadaver in order to determine its resistance to puncture. More precisely, a whole, fresh striped bass (*Morone saxatilis*) fish, a common teleost from the northern Atlantic Ocean, was acquired from a local fish store (Montreal, QC, Canada). The fish had a length of about 30 cm. Penetration specimens were prepared by first removing the head and tail of the fish. Then, the fish was cut in half along the dorsal line. One of the halves, which included the spine, bones, muscle, epidermis (about 400μ thick) and scales (about 300μ thick) was placed in a bath of water (Fig. 2a), skin upwards and under the crosshead of a universal tensile machine mounted with a sharp steel needle (radius 35μ). Using the loading machine the needle was then driven into a through the skin of the fish at a rate of about $10 \mu/\text{s}$, while needle displacement and force were recorded. The test was interrupted after the needle fully punctured the skin, characterized by a sharp and significant drop in force. Both load and displacement were then recorded simultaneously as shown in Fig. 2a. Penetration was performed at various skin locations and the mechanical response was evaluated in three cases: (a) when the skin was stripped off all scales (epidermis only), (b) when only one scale at the location of indent was present and (c) when all scales were present. After averaging the response over a number of different locations, the force–deflection curve shown in Fig. 2b were obtained. Generally, results show that the presence of scales increases the penetration resistance of the skin by almost tenfold. The normalized penetration force, often used to compare the performance of body armors (force divided by mass per unit surface area of protection) is $100\text{--}200 \text{ N}/(\text{kg}/\text{m}^2)$ for fish scales, which is comparable to Kevlar fabric (Termonia, 2006). This is a remarkable performance considering the relatively weak constituents of fish scales (soft collagen and brittle mineral); this gives a hint on the performances that could be achieved in a biomimetic artificial system based on stronger constituents. Interestingly, when all scales except the target scale are removed, the slope of the force–displacement decreases, suggesting some type of collective mechanism involving scales adjacent to the contact point. A thorough understanding of mechanisms responsible for this behavior can be accessed via the numerical strategy devised in this paper.

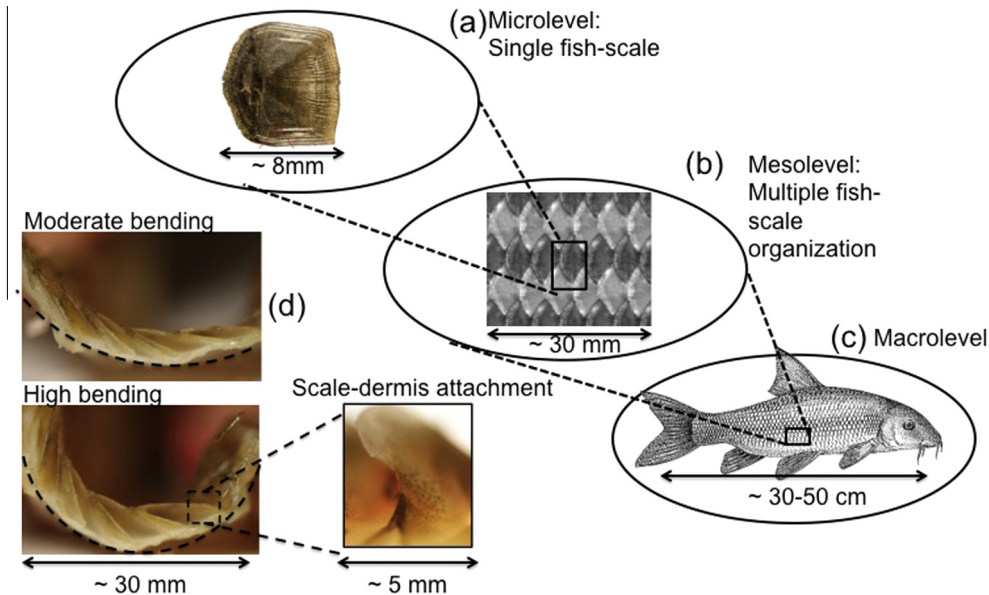


Fig. 1. Structure of fish skin from the micro (single fish-scale) to the macro-level (full skin). Bottom left figures displays the fish skin deformation during bending: a significant rotation of individual scales is typically observed.

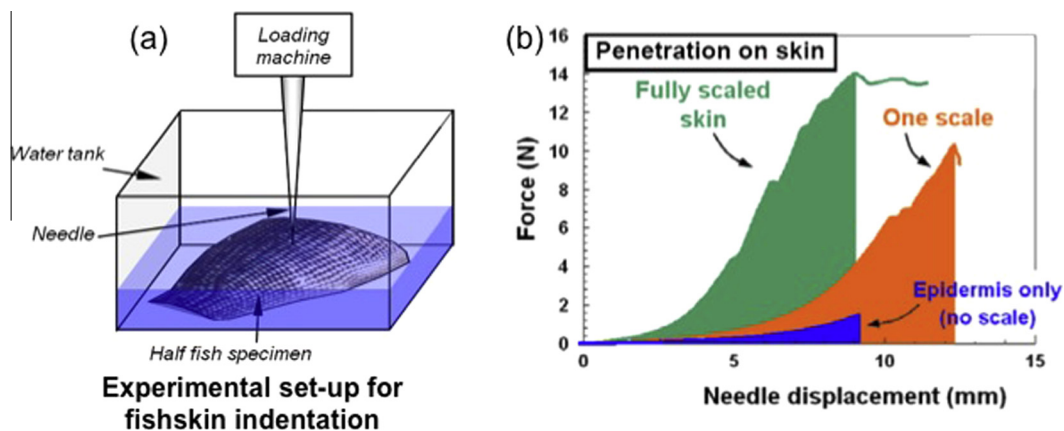


Fig. 2. Illustration of the indentation test and results performed on fish skin.

2.2. A computational approach to study fish skin

Computational studies are ideally suited to assist and guide experimental efforts and determine the influence of a microstructure on the overall behavior of materials (Farsad et al., 2010; Vernerey and Farsad, 2011; Vernerey et al., 2006). A number of issues, however, arise from the fact that the length-scale at which microstructural details are found is usually much smaller than the length-scale of the component. For instance, the indentation of fish skin does not only involve the interaction of a large number of fish scales but is also highly dependent on the detailed topology, properties and friction properties of each individual scale. As a consequence, the modeling becomes very expensive, if not unpractical. To overcome this issue, we adopt a micro-mechanics approach in which the mechanical response of a small representative microstructural element is averaged to yield a macroscopic material response. While not the object of this paper, the latter may be used in conjunction with classical continuum mechanics to assess the material response at the application level. We derive here a homogenization procedure that relies on the three following stages: (a) construction of a representative volume element (RVE), taking advantage of the structure periodicity, (b)

development of a numerical homogenization strategy that enables the computation of averaged stress and strain over the RVE and (c) establishment of a relationship between overall stress (and bending moments) and strain (and curvatures) to assess the role of the microstructure on the response. In this study, we choose to concentrate on the bending moment/curvature relationship as it is the major deformation mode during indentation and natural fish swimming.

The homogenization scheme described in this paper relies on the definition of a representative volume element (RVE) of fish skin. Taking advantage of the periodicity of the scale arrangement (Fig. 3a), it is possible to introduce a periodic cell (the smallest volume the microstructure may be constructed from) which coincides with the definition of an RVE. Referring to Fig. 3b, the intricate fish scale pattern is organized in two rows that run along common horizontal and vertical lines. The nomenclatures given to these two sets are *Prime* and *Double-Prime* which are appear in dark and light shades respectively in Fig. 3b. The reasoning for this method is that *Primes* and *Double Primes* have the same arrangement but are symmetrically offset by a certain displacement. An individual fish scale is superimposed on Fig. 3a in order to visualize the size of the scale with respect to the visible pattern. This

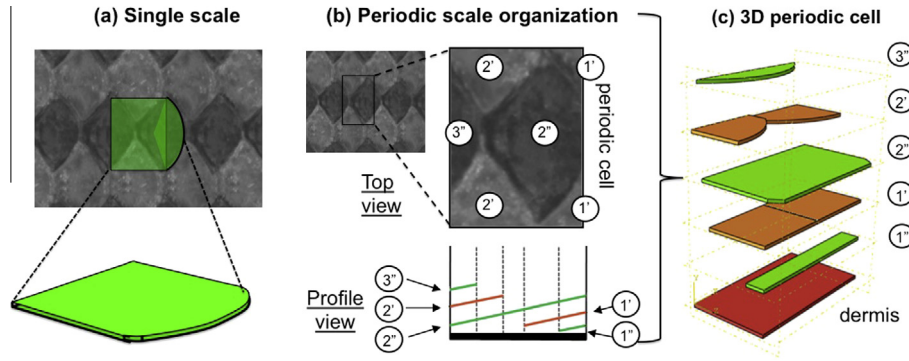


Fig. 3. Construction of the periodic unit cell representative of the fish skin. (a) Representation of the scale assembly viewed from the top, together with the layout of a single scale (in green). Note that only a fraction of the scales' surface is exposed (or visible) due to their high overlap. (b) Due to its periodic organization, the scaled structure can be represented by a periodic cell which contains overlapping sections of seven adjacent scales. According to their position, these scales are labeled by numbers with "prime" and "double prime" referring to the row they belong to (shown in light and dark areas). To better understand the organization of these scales, a profile view of the periodic cell is also presented, where the orientation angle of scales has been exaggerated for clarity. (c) A three-dimensional, exploded view of the periodic cell with corresponding labels. Scales 1'' and 1' are attached to the dermis at their base, on the left side of the schematic, while scales 2'' and 2' may be seen as the continuation of scales 1'' and 1' starting from the left. Similarly, scale 3'' is the continuation of scale 2'' starting from the left. (For interpretation of the references to colour in this figure legend, the reader is referred to the web version of this article.)

analysis permits the determination of the periodic cell, as shown in Fig. 3b in the profile view for which five overlapping scale layers are identified: two *Prime* scale and three *Double Primes* scales. When represented in three-dimension, the periodic cell contains seven different scales that belong to five overlapping layers (Fig. 3c). In examining the three-dimensional assembly, the only portions of scales exposed are the top layer of *Double Prime* scales (3'') and the central scale of the top layer of the *Prime* scales (2'). The bottom layers of the *Prime* and *Double Prime* scales (1' and 1'') are in essence the lower end of the scales that attach to the skin of the fish. In terms of size and geometry, a typical scale from the *Morone saxatilis* has a circular shape with a diameter of 0.8 cm. Size and shape, however, greatly differs from fish to fish, leading to a RVE that is specific to each fish species. We note that differences in RVE geometry, together with differences in the material properties of individual scales, may lead to large variations in the mechanical response of different fish skins.

3. Establishing the structure–property relation

3.1. Homogenization of composite plates based on fish skin

From a macroscopic view-point, fish skin can be approximated as a homogeneous thin shell undergoing large flexural (bending and twisting) deformation whose mechanical behavior can be described by the Kirchhoff–Love shell theory. Kinematics are therefore entirely captured by two quantities, the macroscopic linear strain $\mathbf{E} = [E_{xx} E_{yy} E_{xy}]^T$ and the macroscopic curvature $\mathbf{K} = [K_{xx} K_{yy} K_{xy}]^T$, which satisfy, respectively:

$$\mathbf{E} = \begin{bmatrix} u_{x,x} & u_{x,y}/2 \\ u_{y,x}/2 & u_{y,y} \end{bmatrix} \quad \text{and} \quad \mathbf{K} = \begin{bmatrix} \theta_{y,x} & \theta_{y,y}/2 \\ \theta_{x,x}/2 & \theta_{x,y} \end{bmatrix} \quad (1)$$

with $\mathbf{u}(x,y)$ and $\boldsymbol{\theta}(x,y)$ the in-plane displacement and rotation fields evaluated in a local Cartesian coordinate system (x,y,z) . The associated energy conjugate internal forces are then given by the macroscopic internal stress tensor $\boldsymbol{\Sigma}$ and bending moment \mathbf{M} such that the flexural response of the fish scale assembly is characterized by the relationships:

$$\mathbf{M} = \mathbf{M}(\mathbf{K}), \quad \boldsymbol{\Sigma} = \boldsymbol{\Sigma}(\mathbf{E}). \quad (2)$$

The relation is established by performing average operations of the microscopic curvature $\boldsymbol{\kappa}$ and strain $\boldsymbol{\epsilon}$ and their associated

microscopic stress $\boldsymbol{\sigma}$ and flexural moment \mathbf{m} over the periodic cell described in the previous section. We can generally write:

$$\mathbf{K} = \frac{1}{|\Omega|} \int_{\Omega} \boldsymbol{\kappa}(\mathbf{x}) d\Omega \quad \text{and} \quad \mathbf{E} = \frac{1}{|\Omega|} \int_{\Omega} \boldsymbol{\epsilon}(\mathbf{x}) d\Omega \quad (3)$$

$$\mathbf{M} = \frac{1}{|\Omega|} \int_{\Omega} \mathbf{m}(\mathbf{x}) d\Omega \quad \text{and} \quad \boldsymbol{\Sigma} = \frac{1}{|\Omega|} \int_{\Omega} \boldsymbol{\sigma}(\mathbf{x}) d\Omega \quad (4)$$

where Ω represents the periodic cell domain and $|\Omega|$ is the volume of the domain. In particular, macroscopic and macroscopic quantities are related by the Hill–Mandel condition:

$$\frac{1}{|\Omega|} \int_{\Omega} (\boldsymbol{\sigma} : \delta\boldsymbol{\epsilon} + \mathbf{m} : \delta\boldsymbol{\kappa}) d\Omega = \boldsymbol{\Sigma} : \delta\mathbf{E} + \mathbf{M} : \delta\mathbf{K} \quad (5)$$

which imposes that the variations of macroscopic and microscopic energies are equal. In the present framework, the deformation of the periodic cell is given by writing the relationship between macroscopic curvature \mathbf{K} and microscopic rotations $\hat{\boldsymbol{\theta}}$ as a first-order approximation:

$$\boldsymbol{\theta} = \begin{Bmatrix} \theta_y \\ \theta_x \end{Bmatrix} = \mathbf{K} \begin{Bmatrix} x \\ y \end{Bmatrix} + \begin{Bmatrix} \hat{\theta}_y \\ \hat{\theta}_x \end{Bmatrix} \quad (6)$$

$$\mathbf{u} = \begin{Bmatrix} u_x \\ u_y \end{Bmatrix} = (\mathbf{E} - \mathbf{K}\mathbf{z}) \begin{Bmatrix} x \\ y \end{Bmatrix} + \begin{Bmatrix} \hat{u}_x \\ \hat{u}_y \end{Bmatrix} \quad (7)$$

where x and y are microscopic positions in a Cartesian coordinate system associated with the undeformed periodic cell and the vectors $\hat{\boldsymbol{\theta}}$ and $\hat{\mathbf{u}}$ are fluctuating fields that do not trigger any macroscopic deformations and curvatures. An important aspect of computational homogenization is the nature of the boundary conditions applied on the RVE. In general, the boundary conditions should account for the existence of material around the unit cell. In the present situation, this feature is facilitated by the fact that the periodicity of the unit cell is conserved throughout its deformation history. Applying such conditions on domains undergoing a combination of bending and in-plane deformation is not trivial, mainly due to the fact that displacement and rotation are strongly coupled fields. We hence introduce a formulation that may be summarized as follows. As depicted in Fig. 4, the boundaries of the periodic cell are decomposed into left/right and front/back sides. Two corresponding points on opposite sides of a unit cell are then subjected to the following constraints in terms of rotation $\hat{\theta}$ measured in a local coordinate system that is tangent to the deformed shell:

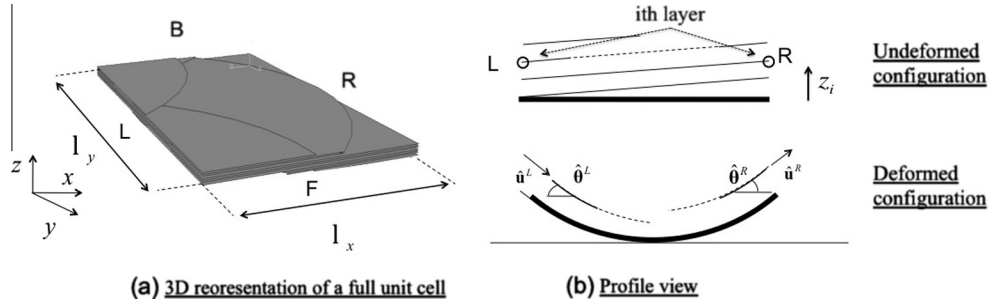


Fig. 4. (a) Three-dimensional representation of the periodic cell, its associated coordinate system and the decomposition of its boundaries into left (L), right (R), back (B) and front (F) sections. (b) Profile view of the periodic cell in the undeformed and deformed (bent) configuration. Particular attention is brought to the i th layer (third on the schematic) for which the corresponding left and right material points are shown with circles. Relative to the base dermis layer, these points are located at coordinate z_i . Their rotation angles $\hat{\theta}$ and displacement vectors $\hat{\mathbf{u}}$, illustrated here in the deformed configuration, are related by the periodic boundary conditions expressed in (8) and (9).

$$\Theta = \begin{Bmatrix} \hat{\theta}_x^R - \hat{\theta}_x^L \\ \hat{\theta}_y^R - \hat{\theta}_y^L \\ \hat{\theta}_x^F - \hat{\theta}_x^B \\ \hat{\theta}_y^F - \hat{\theta}_y^B \end{Bmatrix} = \underbrace{\begin{bmatrix} 0 & 0 & \ell_x/2 \\ \ell_x & 0 & 0 \\ 0 & \ell_y & 0 \\ 0 & 0 & \ell_y/2 \end{bmatrix}}_{\mathbf{B}} \lim_{\mathbf{A}} \begin{Bmatrix} K_{11} \\ K_{22} \\ K_{12} \end{Bmatrix}, \quad (8)$$

where the length ℓ_x and ℓ_y refer to the dimension of the unit cell as shown in Fig. 4. Similarly, the displacement vectors $\hat{\mathbf{u}}$ of two points that belong to i th layer (referring to Fig. 4) are such that:

$$\mathbf{U}^i = \begin{Bmatrix} \hat{u}_x^R - \hat{u}_x^L \\ \hat{u}_y^R - \hat{u}_y^L \\ \hat{u}_x^F - \hat{u}_x^B \\ \hat{u}_y^F - \hat{u}_y^B \end{Bmatrix} = \underbrace{\begin{bmatrix} \ell_x & 0 & 0 \\ 0 & 0 & \ell_x/2 \\ 0 & 0 & \ell_y/2 \\ 0 & \ell_y & 0 \end{bmatrix}}_{\mathbf{B}} \left(\begin{Bmatrix} E_{11} \\ E_{22} \\ E_{12} \end{Bmatrix} - z_i \begin{Bmatrix} K_{11} \\ K_{22} \\ K_{12} \end{Bmatrix} \right) \quad (9)$$

where z_i is the out-of-plane distance of a point on the i th layer from the neutral axis (taken to be the dermis in our study). The first condition ensures that the unit cell undergoes a macroscopic curvature in a periodic fashion while the second condition enforces periodicity in tangential displacements. The macroscopic bending and twisting moments are then found by invoking the principle of virtual work as follows:

$$\int_{\Omega} (\boldsymbol{\sigma} : \delta \boldsymbol{\epsilon} + \mathbf{m} : \delta \boldsymbol{\kappa}) d\Omega = \sum_{i=1}^n (\mathbf{f}^i \cdot \delta \mathbf{U}^i) + \boldsymbol{\mu} \cdot \delta \Theta \quad (10)$$

where the right hand side denotes the variation of internal energy in the periodic cell, while the left hand term represents the variation of external work provided by the reaction force $\mathbf{f}^i = [f_x^{i,RL} f_y^{i,RL} f_x^{i,FB} f_y^{i,FB}]^T$ and $\boldsymbol{\mu} = [\mu_x^{i,RL} \mu_y^{i,RL} \mu_x^{i,FB} \mu_y^{i,FB}]^T$ associated with the imposed periodic boundary conditions. Using the Hill-Mandel condition (5) and the fact that $\delta \Theta = \mathbf{A} \delta \mathbf{K}$ from (8), we can obtain the macroscopic stress and bending moment through the following equality:

$$\boldsymbol{\Sigma} = \frac{\mathbf{B}^T}{\ell_x \ell_y} \sum_{i=1}^n \mathbf{f}^i \quad \text{and} \quad \mathbf{M} = \frac{1}{\ell_x \ell_y} \left(\mathbf{A}^T \boldsymbol{\mu} - \mathbf{B}^T \sum_{i=1}^n z_i \mathbf{f}^i \right) \quad (11)$$

in which the matrices \mathbf{A} and \mathbf{B} were introduced in (8) and (9). It is clear here that the overall stress only has contributions from applied forces on the boundary nodes while the overall moment comprises both the applied moments and the moments from the applied forces about the neutral plane.

3.2. Implementation and computational aspects

In practice, the homogenization equations presented in (8), (9) and (11) can be implemented within the finite element method or other appropriate numerical techniques. In the present work,

we use the commercial software ABAQUS© and discretize the three-dimensional unit cell with Kirchhoff–love plate elements (for scales) and membrane elements (for the dermis) with thickness 0.01 and 0.03 cm, respectively (Fig. 5). The equations are solved using an implicit, static solver and the response of the periodic cell is estimated for various increments of macroscopic curvature. The contact constraints are enforced using the Penalty method and the periodic boundary conditions are enforced by non-linear multi-point constraints, based on the Lagrange multiplier method that enforce the prescribed relative displacement of a pair of nodes on opposite boundaries. The convergence of the scheme was ensured by choosing an element size so that results were independent of discretization. The computational homogenization procedure can be summarized as follows:

1. The overall curvature and strain are imposed by prescribing the rotation and displacement on the edges. More specifically, the overall values of the strain \mathbf{E} and curvature \mathbf{K} are first imposed and the corresponding displacements and rotations on the unit cell's boundaries are computed by enforcing Eqs. (8) and (9) with the Lagrange multiplier method. As discussed above, this method ensures that the cell deformation remains periodic at all time.
2. The equilibrium of the periodic cell is computed for each increment using the implicit FEM solver.
3. The overall moments are determined by computing the reaction forces $\boldsymbol{\mu}$ and \mathbf{f}^i (identified with Lagrange multipliers) and using (11).
4. The operation is repeated by increasing the imposed curvature in order to obtain the overall moment/curvature relationship.

4. Results and discussion

This section discusses the computational homogenization of two types of fish scale structures: (a) a simple one-dimensional scale organization, as shown in Fig. 5a, that serves as a reference or comparison purposes and (b) the more realistic scale shape and organization of the *Morone saxatilis* (Fig. 5b).

4.1. Micro-scale parameters and material models

Fish scales: Typically, because individual scales exhibit a very large surface/thickness ratio, they can be modeled as Kirchhoff plate structures. Furthermore, individual scales are assumed to be isotropic and to behave in a linearly elastic fashion. The Young's modulus and Poisson's ratio can then be determined from tensile tests (Zhu et al., 2011) reported in Table 1. It is worth mentioning that these assumptions are coarse since closer observations of fish scales reveal that they are cross-ply laminates composed of two

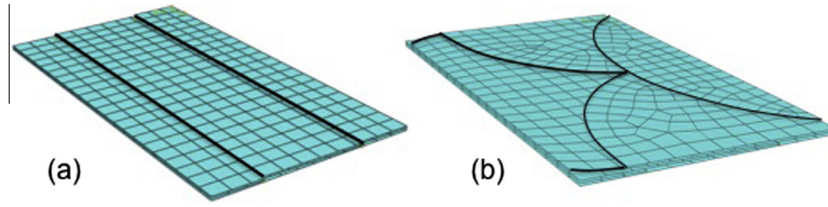


Fig. 5. Geometry and finite element discretization for a simple one-dimensional scale arrangement and the scale configuration observed on *Morone saxatilis*. Both unit cells are periodic.

distinct anisotropic layers, the bony layer and the collagen layer, each layer being laminated (Zhu et al., 2011). However the use of an effective modulus is sufficient for the present study of scale-scale and scale-dermis interactions. Finally, whereas fish-scale typically display small variations in their thickness (Zhu et al., 2011) (they are thicker in the center), we consider the simplifying case of a planar shells with uniform thickness. As a consequence, our simulations may slightly under-estimate their bending stiffness but the general predictions should not be affected by this assumption.

Dermis: The dermis provides a support for the scales and therefore is expected to be a significant influence on the interaction between fish scales during bending and torsion. In addition, when the fish scale structure is stretched, the scales do not participate and the mechanical response is solely due to the dermis. In that respect, the properties of the dermis may be critical to the indentation of the fish scale structure. The dermis may be viewed as a membrane undergoing finite deformation due to its lower modulus. As a first approximation, an incompressible Neo-Hookean material model is used whose properties are determined from curve fitting the indentation tests of the skin without scales (Fig. 2). The relationship between the Cauchy stress σ and the Green–Lagrange deformation tensor ϵ of the membrane is given in terms of the Neo-Hookean strain energy function ψ as:

$$\sigma = \frac{1}{J} \mathbf{F} \cdot \frac{\partial \psi}{\partial \epsilon} \cdot \mathbf{F}^T \quad \text{and} \quad \psi = C(I_1 - 3) \quad (12)$$

where \mathbf{F} is the deformation gradient, I_1 and $J = \det(\mathbf{F})$ are respectively the first strain invariant and the jacobian of the deformation, and C is the shear modulus of the dermis (Table 1). Note that $J = 1$ due to the incompressibility of the material.

Scale-scale and dermis-scale interactions: These interactions are comprised of contact, which arise from the conditions that two materials do not penetrate each other and friction, which depends on the surface properties of scales and skin. Interestingly, live fish possess a viscous mucus on the scales surface whose presence may be accounted by considering a very low friction coefficient between adjacent scales (Zhu et al., 2013). Another type of interaction arises from the existence of a thin layer of dermis overlapping each scale over a distance that can span as much as half of the scale length. This layer acts to resist rotation of a scale with respect to the underlying dermis as shown in Fig. 1.d. Mechanically, this constraint is equivalent to a distributed torsional spring linking the base of each scale to the dermis, with stiffness k_d , measured per

Table 1
Parameters used in the simulations (Zhu et al., 2011).

Definition	Symbol	Value	unit
Scale Young modulus	E_s	2.2	GPa
Scale thickness	h	0.3	mm
Scale Poisson's ratio	ν_s	0.45	n/a
Shear modulus of the dermis	C	10	kPa
Width of unit cell	ℓ_x	0.27	cm
Length of unit cell	ℓ_y	0.53	cm

unit length (Fig. 6). We will show below that this element plays a significant role on the overall behavior of the skin.

4.2. Mechanical response of a simplified one-dimensional scale arrangement

The simplified fish scale arrangement presented in Fig. 5a serves two purposes. First, it is used to validate our three-dimensional model against the predictions of a two-dimensional model of fish scale bending obtained previously in Vernerey and Barthelat (2010). Second, it is used to gain insights on the behavior on such structures in order to provide a reference with which to compare the response of more complex scale organizations. It was found in Vernerey and Barthelat (2010) that the normalized rotational stiffness $K_d = k_d \ell / EI$ of the scale-dermis attachment plays a significant role in the response of the composite skin. Here, E is the Young's modulus of the scale (Table 1), $I = 2h^3/3(1 - \nu_s^2)$ is the moment of inertia of the cross-section and ℓ is the length of a scale. We thus propose to analyse the overall moment–curvature response of the skin for different values of k_d . Our first study consists of assessing the average response of the skin for longitudinal bending (the bending axis is parallel to the line of scale-dermis attachments) as depicted in Fig. 7. The computational homogenization scheme presented in the previous section leads to very satisfactory results as the unit cell remains entirely periodic regardless of the degree of bending and the heterogeneity of the micro-scale deformations and rotation. This can be clearly seen by observing the cross-section of the unit cell as it deforms (Fig. 7) in which the juxtaposition of unit cells clearly displays a continuous rotation and displacement across their boundary. The overall moment–curvature relationship was then computed using (11) as shown in Fig. 8a, where κ denotes the normalized curvature K_x/ℓ_x . In agreement with our previous one-dimensional study (Vernerey and Barthelat, 2010), results show that the bending response of the skin is very sensitive to the rigidity K_d scale-dermis attachment. For large values of K_d , scale bending is the preferred mode of deformation (Fig. 8a, and the moment–curvature response becomes essentially linear with an overall stiffness equal to:

$$K_h = EI/r \quad (13)$$

where EI is the bending rigidity of individual scales and the quantity r is the ratio of the spacing and length of scale ($r = 1/2$ in our study). When K_d decreases (Fig. 8e and f), it is observed that the elastic response transitions to a very nonlinear bending stiffening behavior that is eventually dominated by the rotation of individual scales (Fig. 8.f). In this case, one can decompose the moment–curvature in three regions. For small bending regimes, the local deformations primarily involves scale rotation, a feature that is responsible for the low bending stiffness of the skin. For intermediate curvatures, scale rotation becomes increasingly harder due to geometrical



Fig. 6. Illustration of the various parts and idealization of the fish skin composite.

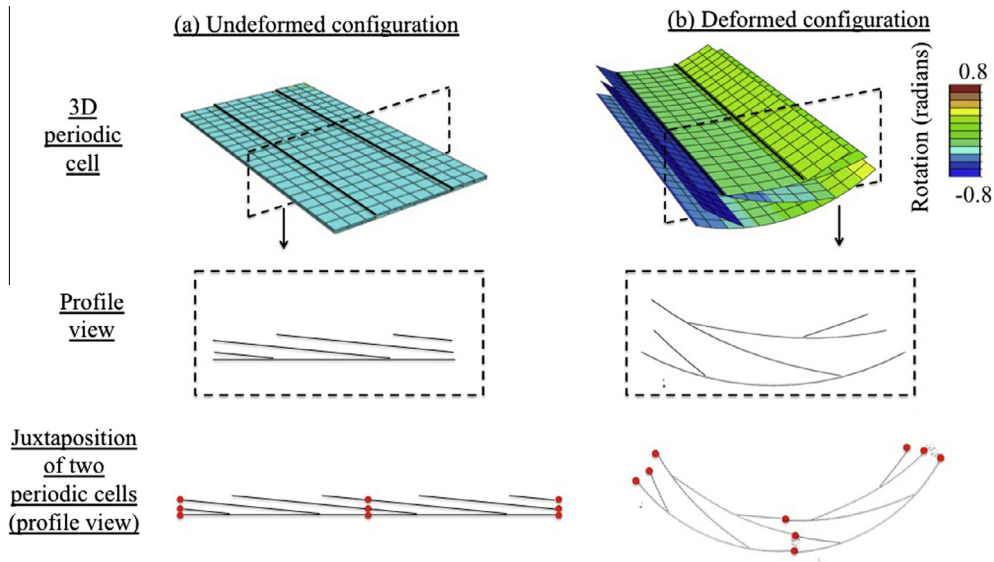


Fig. 7. (a) Undeformed and (b) deformed configurations of the simplified scale arrangement for a rotational spring stiffness $K_d = 0.1$ and a scale overlap ratio $r = 1/2$. The three-dimensional representation may be better understood by looking at the profile view, in which the scale angle has been exaggerated in the undeformed configuration. The juxtaposition of two periodic cells is also shown to illustrate how the periodicity of the structure is conserved during deformation. We note here that the boundary nodes (left and right) are represented by solid circles.

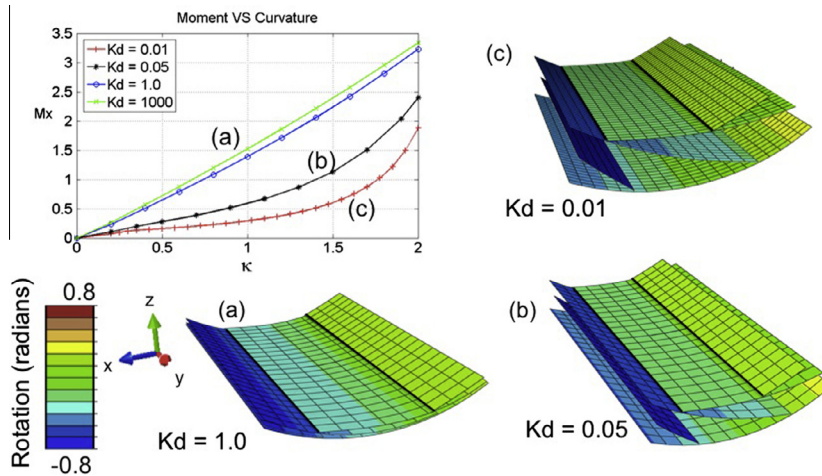


Fig. 8. (a) Longitudinal moment–curvature response (M_x versus κ_x) and corresponding three-dimensional deformation patterns for a scale overlap ratio of $r = 1/2$ and different values of normalized scale–dermis rigidity K_d . It can be seen that scale bending is dominant for large K_d while scale rotation is preponderant for small K_d . The latter is responsible for the observed stiffening response of the structure.

constraints, yielding an overall stiffening of the skin. Finally, for higher curvatures ($\kappa \approx 1$), a phenomenon interpreted as scale locking, precludes any additional rotation; this ultimately results in a deformation regime dominated by scale bending and its associated high stiffness.

The skin response to lateral bending displays a very different behavior. Indeed, in this direction, scale rotation is obviously not activated and the only mode of deformation is bending. As a consequence, neither the local deformation fields nor the overall mechanical behavior of the skin are sensitive to differences in scale–dermis rigidities (Fig. 9). The behavior of the skin can thus be described as that of a homogeneous shell whose stiffness K_h is defined in (13).

4.3. Mechanical response of biological fish skin: case of *Morone saxatilis*

Natural fish skin differs from the above example in that it has a more elaborate and intricate structure. It is therefore of interest to

understand if the mechanisms observed in the simplified structure are similar in natural systems or if new phenomena emerge. Our first study therefore consists in studying the response in longitudinal bending as it is the natural mode of deformation during fish swimming. As shown in Fig. 10, the results display a response that is very similar to the homogeneous one-dimensional structure above. As the value of K_d decreases, we observe a transition of a deformation mode dominated by scale bending to one that is dominated by scale rotation. In the latter case, this mechanism yields the typical bending stiffening response discussed earlier. By comparing the moment curvatures in Figs. 10 and 8, it can be seen that the bending stiffening is however not as pronounced, a feature that can be explained by fish scale morphology. Indeed, simulations clearly show that during longitudinal bending, the contact region mostly localizes at the narrow tip of individual scales; this triggers a strong bending concentration at the tip, even for small values of the scale-attachment stiffness K_d . Such inhomogeneities in scale deformation tends to reduce the total amount of scale rotation

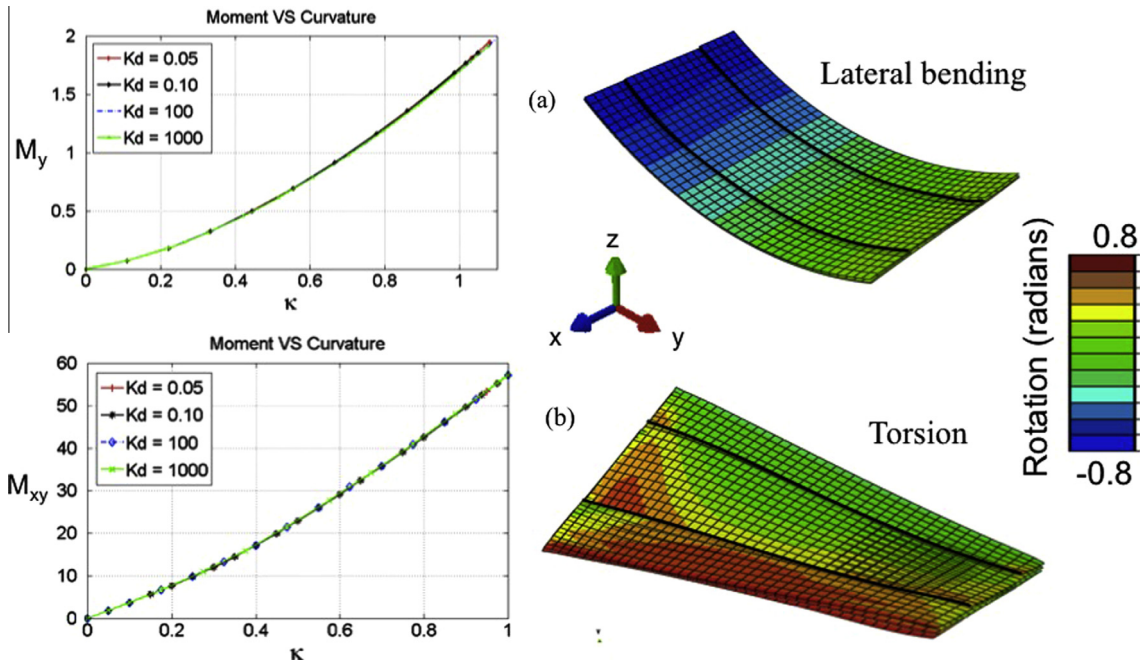


Fig. 9. Moment–curvature response for lateral bending for different values of normalized scale-dermis rigidity.

and thus the associated stiffening characteristics in the overall response. We note, however, that these effects can be reduced by considering a slightly non-planar scale geometry (a feature that can actually be observed in most teleost scales), which could significantly affect its bending properties. This aspect of the problem is left for future studies.

We next investigated the lateral bending and torsional behavior of the skin as shown in Fig. 11. Interestingly, we found that these modes of deformation are completely insensitive to the scale attachment rigidity K_d , and thus, the behavior was that of a homogeneous plate. This result is confirmed by the observation of a fairly homogeneous scale deformation (Fig. 11a and b) with no scale rotation, even at negligible values of K_d . In other words, the deformation is entirely constrained by geometrical constraints (contact) and the presence of scales is not apparent in the overall composite behavior. A consequence of this behavior is that the skin appears much stiffer in the lateral direction than in the longitudinal direction in the range of low to moderate bending. Our simulations therefore confirm that fish skin is a strongly anisotropic shell

for which the *bending stiffening* capability is only observed for longitudinal bending but neither in lateral bending nor in torsional deformation modes.

Overall, our numerical study shows that fish scales display very strong nonlocal interactions that are responsible for the mechanical resistance of the skin against localized bending. This feature is mainly due to an overlapping organization that enables them to *share the load via an interlocking mechanism* and thus redistribute bending deformation of large areas. It is therefore not surprising that the force–deflection curve of intact fish skin displays a significantly higher stiffness compared to a skin deprived of scales as observed in our experimental study of Fig. 2.

5. Summary and discussion

As a summary, our paper presented a computational methodology to analyze the mechanical behavior of thin composite structures with a direct application to fish skin. We have shown that similar to bulk materials, homogenization of composite shells

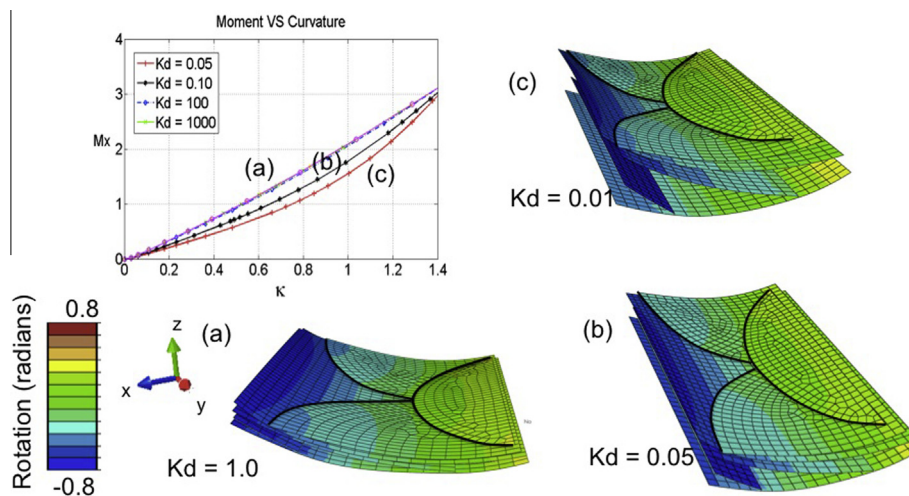


Fig. 10. Longitudinal bending response of a natural fish skin for three values of scale-dermis rotational rigidity and associated deformation pattern.

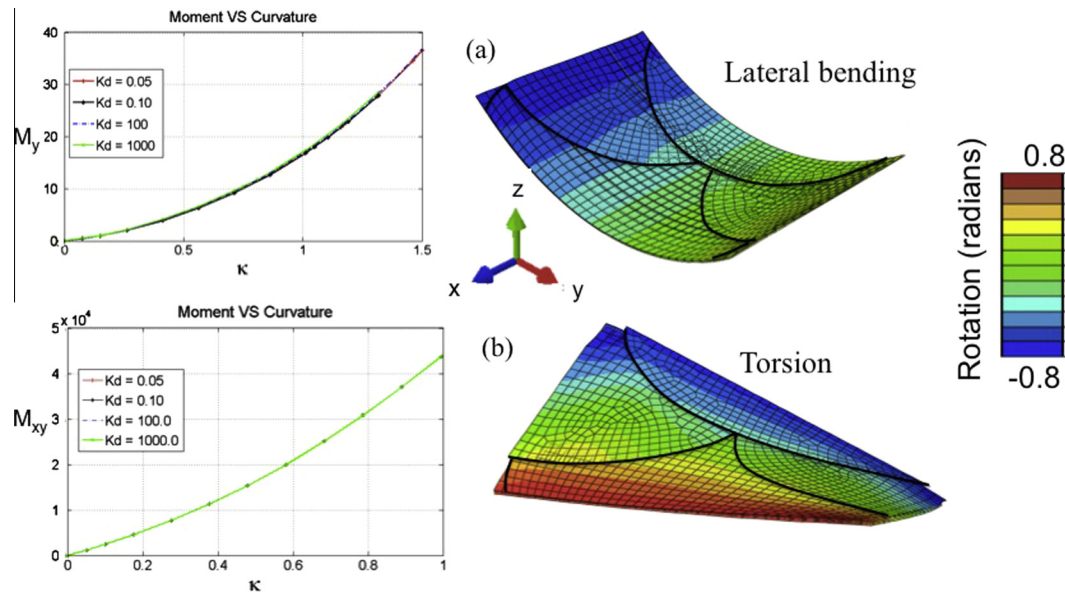


Fig. 11. Lateral bending and torsional response of a natural fish skin for different values of scale-dermis rotational rigidity. These deformation modes are insensitive to K_d as scale rotation is not activated.

results from the determination and analysis of a representative volume element (or a periodic unit cells for periodic structures), which may possess feature in- and out-of-plane. We have described a methodology to computationally determine the overall strain and curvature (with the associated stress and moments) via the application of periodic boundary conditions. The equations were then used to better understand the nonlinear response of fish skin and its relationship with the underlying shell structure (scale morphology, mechanical properties and rigidity of the scale attachment to the dermis). We specifically investigated the bending and torsional response of the skin of a common teleost fish, known as *Morone saxatilis*, in order to better understand the effect of scales on skin mechanics as observed during indentation tests and fish swimming. We have shown that the response was highly anisotropic. Its longitudinal bending response exhibited a characteristic *bending stiffening* response for low scale-dermis rigidity, which seems to be biologically relevant. This nonlinear behavior originates from purely geometric constraints between neighboring scales, which can be tuned by changing the stiffness K_d of the scale-dermis attachments providing a support for the scales. Interestingly, this behavior was not observed for lateral bending and torsional deformation modes, for which scales deformed in a homogeneous fashion without rotating. Through these mechanisms, it seems like the skin accomplishes two important structural goals: (a) provide a rigid armor that protects the fish against potential puncture loads arising from predator attacks and (b) preserve freedom of motion by remaining relatively compliant. The scaled structure of the skin provides a simple and highly efficient way to achieve these a priori incompatible properties by exhibiting a very stiff behavior in deformation modes that are not physiological (torsion and lateral bending) and when the deformation is out of the physiological range (very high longitudinal bending curvatures). For moderate longitudinal bending however, the skin exhibits a very flexible response which stiffens as the radius of curvature becomes close to the size of individual scales. This behavior is obtained by allowing scales to rotate with respect to the dermis, which is energetically more favorable than scale bending. For high bending deformation, normal contact forces between scales become increasingly large and eventually prevents scale rotation, a phenomenon that we denoted as *scale locking*.

While the biological relevance of these results would necessitate more experimental tests on live fish, their impact may be important in the replication of fish skin mechanisms in thin, flexible engineering materials. Indeed, the scaled-structure of fish skin is an intriguing membrane system that displays a rich spectrum of mechanical responses due to a subtle arrangement of building blocks (scale, dermis, pockets) and that is highly adaptable as a function of specific biological or engineering functions (such as external tendon and armor protection). The domain of applications of scaled structures could therefore span many engineering applications, from ultra-light and flexible armor systems to important future technological development including flexible electronics or the design of smart and adaptive morphing structures for aerospace vehicles. Many key research and technology advances may therefore be positively affected by a stronger effort in the study of this intriguing material system.

Acknowledgments

The authors wish to acknowledge the support of the National Science Foundation under award CMMI 0927585. In addition, we wish to thank Yevgeniy Kaufman for his help in building the geometry of the periodic cell for fish skin.

References

- Aizenberg, J., Weaver, J., Thanawala, M., Sundar, V., Morse, D., Fratzi, P., 2005. Skeleton of euplectella sp.: structural hierarchy from the nanoscale to the macroscale. *Science* 309, 275–278.
- Barthelat, F., 2012. Nacre from mollusk shells: a model for high-performance structural materials. *Bioinspiration and Biomimetics* 5, 1–8 (Special issue on the biomimetics of aquatic life: applications for engineering).
- Barthelat, F., Tang, H., Zavattieri, P., Li, C., Espinosa, H., 2007. On the mechanics of mother-of-pearl: a key feature in the material hierarchical structure. *Journal of the Mechanics and Physics of Solids* 55, 225–444.
- Bruet, B., Song, J., Boyce, M., Ortiz, C., 2008. Materials design principles of ancient fish armour. *Nature materials* 7, 748–756.
- Chen, P., Schirer, J., Simpson, A., Nay, R., Lin, Y., Yang, W., Lopez, M., Li, J., Olevsky, E., Meyers, M.A., 2011. Predation versus protection: fish teeth and scales evaluated by predation versus protection: fish teeth and scales evaluated by nanoindentation. *Journal of Materials Research* 27, 100–112.
- Currey, J., 1999. The design of mineralised hard tissues for their mechanical functions. *Journal of Experimental Biology* 202, 3285–3294.

- Farsad, M., Vernerey, F.J., Park, H.S., 2010. An extended finite element/level set method to study surface effects on the mechanical behavior and properties of nanomaterials. *International Journal of Numerical Methods in Engineering* 84, 1466–1489.
- Hebrank, M.R., 1980. Mechanical-properties and locomotor functions of eel skin. *Biological Bulletin* 158, 58–68.
- Hebrank, M.R., Hebrank, J.H., 1986. The mechanics of fish skin – lack of an external tendon role in 2 teleosts. *Biological Bulletin* 171, 236–247.
- Jawad, L.A., 2005. Comparative morphology of scales of four teleost fishes from sudan and yemen. *Journal of Natural History* 39, 2643–2660.
- Long, J.H., Adcock, B., Root, R.G., 2002. Force transmission via axial tendons in undulating fish: a dynamic analysis. *Comparative Biochemistry and Physiology a-Molecular and Integrative Physiology* 133, 911–929.
- Meyers, M.A., Lin, A.Y.M., Seki, Y., Chen, P.Y., Kad, B.K., Bodde, S., 2006. Structural biological composites: an overview. *JOM: Journal of the Minerals, Metals & Materials Society* 58, 35–41.
- Sudo, S., Tsuyuki, K., Ito, Y., Ikehagi, T., 2002. A study on the surface shape of fish scales. *JSME International Journal Series C-Mechanical Systems Machine Elements and Manufacturing* 45, 1100–1105.
- Tang, Z., Kotov, N., Magonov, S., Ozturk, B., 2003. Nanostructured artificial nacre. *Nature Materials* 2, 413–418.
- Termonia, Y., 2006. Puncture resistance of fibrous structures. *International Journal of Impact Engineering* 32, 1512–1520.
- Vernerey, F., Barthelat, F., 2010. On the mechanics of fishscale structures. *International Journal of Solids and Structures* 47, 2268–2275.
- Vernerey, F., Farsad, M., 2011. A constrained mixture approach to mechano-sensing and force generation in contractile cells. *Journal of the Mechanical Behavior of Biomedical Materials* 4, 1683–1699.
- Vernerey, F., McVeigh, C., Liu, W., Moran, B., Tewari, D., Parks, D., Olson, G., 2006. The 3-d computational modeling of shear-dominated ductile failure in steel. *JOM, The Journal of The Minerals, Metals and Materials Society*, 433–445.
- Vincent, J.F.V., Bogatyreva, O.A., Bogatyrev, N.R., Bowyer, A., Pahl, A.K., 2006. Biomimetics: its practice and theory. *Journal of the Royal Society Interface* 3, 471–482.
- Vogel, S., 2000. *Cats' Paws and Catapults: Mechanical Worlds of Nature and People*. W.W. Norton and Company.
- Zhu, D., Ortega, C., Motamedi, R., Szewciw, L., Vernerey, F., Barthelat, F., 2011. Structure and mechanical performance of a “modern” fish scale. *Advanced Biomaterials* 14, B185–B194.
- Zhu, D., Barthelat, F., Vernerey, F., 2012. The intricate multiscale mechanical response of natural fish-scale composites. *Handbook of Micromechanics and Nanomechanics*, Pan Stanford Publishing Co, in press.
- Zhu, D., Szewciw, L., Vernerey, F., Barthelat, F., 2013. Puncture resistance of the scaled skin from striped bass: collective mechanisms and inspiration for new flexible armor designs. *Journal of the Mechanical Behavior of Biomedical Materials* 24, 30–40.